

# Strong decays of nonstrange $q^3$ baryons

R. Bijker

Instituto de Ciencias Nucleares, U.N.A.M.,  
A.P. 70-543, 04510 México, D.F., México

F. Iachello

Center for Theoretical Physics, Sloane Laboratory,  
Yale University, New Haven, CT 06520-8120, U.S.A.

A. Leviatan

Racah Institute of Physics, The Hebrew University,  
Jerusalem 91904, Israel

## Abstract

We study strong decays of nonstrange baryons by making use of the algebraic approach to hadron structure. Within this framework we derive closed expressions for decay widths in an elementary-meson emission model and use these to analyze the experimental data for  $N^* \rightarrow N + \pi$ ,  $N^* \rightarrow \Delta + \pi$ ,  $N^* \rightarrow N + \eta$ ,  $\Delta^* \rightarrow N + \pi$ ,  $\Delta^* \rightarrow \Delta + \pi$  and  $\Delta^* \rightarrow \Delta + \eta$  decays.

PACS numbers: 13.30.Eg, 11.30.Na, 14.20.Gk

# I Introduction

A large amount of experimental data was accumulated in the 1960's and 1970's on the spectroscopy of light hadrons. These data led first to the introduction of  $SU_f(3)$  by Gell'Mann [1] and Ne'eman [2] (later enlarged to  $SU_{sf}(6)$  by Gürsey and Radicati [3]), and subsequently to  $SU_c(3)$  color symmetry as a gauge symmetry of strong interactions. The construction of dedicated facilities (*e.g.* CEBAF, MAMI, ELSA) that promise to produce new and more accurate data on the same subject, have stimulated us to revisit baryon spectroscopy with the intent to reexamine whether or not the new data can shed some new light on the structure of hadrons. In this reanalysis we have introduced, in addition to the basic spin-flavor-color symmetry,  $SU_{sf}(6) \otimes SU_c(3)$ , a new ingredient, namely a space symmetry,  $\mathcal{G}$ , which we have taken to be  $\mathcal{G} = U(7)$  for baryons [4]. The introduction of the space symmetry allows us to examine, in a straightforward way, several limiting situations (*e.g.* harmonic oscillator and collective dynamics), and to produce transparent results that can be used to analyze the experimental data. This approach has been used [4, 5] to analyze the mass spectrum and electromagnetic couplings of nonstrange baryon resonances. It presents an alternative for the use of nonrelativistic or relativized Schrödinger equations. In addition to electromagnetic couplings, strong decays of baryons provide an important, complementary, tool to study the structure of baryons. These strong couplings are needed to analyze the new upcoming experimental data, especially  $(e, e'\pi)$  and  $(e, e'\eta)$ . Furthermore, we want to understand whether or not unusual features appear in the data, which may point out to 'new' physics, new meaning here unconventional configurations of quarks and gluons, such as hybrid states,  $q^3 - g$ , or multiquark states,  $q^3 - q\bar{q}$ . For example, the observed large  $\eta$  width of the  $N(1535)S_{11}$  resonance has led to considerable discussion [6, 7, 8, 9, 10] about the nature of this resonance.

The strong decays have been analyzed previously in the nonrelativistic [11] and relativized quark models [12]. These models emphasize single-particle aspects of quark dynamics in which only a few low-lying configurations in the confining potential contribute significantly to the baryon wave function. In the framework of the earlier mentioned algebraic approach, it is possible to study also other, more collective, types of dynamics. In this article, we analyze in detail the strong decays in a collective model of baryon structure. The article is organized as follows: in Section II we briefly discuss the method of calculation, in Section III we present the results, which are compared with the existing data in Section IV. Finally, in Section V we present our conclusions and point out some open problems.

## II Method of calculation

We consider in this article strong decays of baryons by the emission of a pseudoscalar meson

$$B \rightarrow B' + M . \tag{1}$$

In order to calculate these decays we need two ingredients: (i) the wave function of the initial and final states and (ii) the form of the transition operator. We write both the wave functions and the transition

operators in algebraic form. We take the wave functions as representations of  $U(7) \otimes SU_{sf}(6) \otimes SU_c(3)$ , as discussed in [4]. The algebraic formulation allows us to study a large class of models, all with the same spin-flavor-color structure, but different types of quark dynamics (*e.g.* single-particle and collective). Each scenario corresponds to different ways in which the  $U(7)$  spatial symmetry is broken down to the angular momentum group  $SO(3)$ . Among the models in this class is the familiar harmonic oscillator quark model characterized by the breaking

$$U(7) \supset U(6) \supset U_\rho(3) \otimes U_\lambda(3) \supset SO_\rho(3) \otimes SO_\lambda(3) \supset SO(3) \supset SO(2) , \quad (2)$$

where the index  $\rho$  and  $\lambda$  refers to the two relative Jacobi coordinates

$$\begin{aligned} \vec{\rho} &= \frac{1}{\sqrt{2}}(\vec{r}_1 - \vec{r}_2) , \\ \vec{\lambda} &= \frac{1}{\sqrt{6}}(\vec{r}_1 + \vec{r}_2 - 2\vec{r}_3) . \end{aligned} \quad (3)$$

The nonrelativistic and relativized quark potential models [13, 14] are formulated in this harmonic oscillator basis.

In a collective model the baryon resonances are interpreted in terms of rotations and vibrations of the string configuration in Fig. 1, which is characterized by the two relative Jacobi coordinates of Eq. (3). The three constituent parts carry the global quantum numbers: flavor = triplet =  $u, d, s$ ; spin = doublet =  $1/2$ ; and color = triplet (we do not consider here heavy quark flavors). Different types of collective models are specified by a distribution of the charge, magnetic moment, etc., over the entire volume. For the present analysis of strong decays we use the (normalized) distribution

$$g(\beta) = \beta^2 e^{-\beta/a} / 2a^3 , \quad (4)$$

where  $\beta$  is a radial coordinate and  $a$  is a scale parameter. We have shown in [5] that the above distribution appears to describe the available data on electromagnetic form factors and helicity amplitudes up to  $Q^2 \approx 10 - 20$  (GeV/c) $^2$ .

The spatial part of the baryon wave functions in the ‘collective’ model is characterized by the following labels:  $(v_1, v_2); K, L_t^P$  [4], where  $(v_1, v_2)$  denotes the vibrations (stretching and bending) of the configuration of Fig. 1;  $K$  denotes the projection of the rotational angular momentum  $L$  on the body-fixed axis;  $P$  the parity and  $t$  the symmetry type of the state under the point group  $D_3$ . The classification under  $D_3$  and parity is equivalent to that of the point group  $D_{3h}$ , which describes the discrete symmetry of the object of Fig. 1. Instead of the  $D_3$  labels ( $t = A_1, A_2, E$ ) one can use the labels of  $S_3$  ( $t = S, A, M$ ), the group of permutations of the three constituent parts ( $S_3$  and  $D_3$  are isomorphic). The permutation symmetry  $t$  of the spatial part of the wave function must be the same as that of the spin-flavor part in order to have total wave functions that are antisymmetric (the color part is a color-singlet, *i.e.* antisymmetric). Therefore one can also use the dimension of the  $SU_{sf}(6)$  representations to label the states:  $A_1 \leftrightarrow S \leftrightarrow 56$ ,  $A_2 \leftrightarrow A \leftrightarrow 20$  and  $E \leftrightarrow M \leftrightarrow 70$ . We adhere to the latter notation and label the states

by

$$| [\dim\{SU_{sf}(6)\}, L^P]_{(v_1, v_2); K} \rangle . \quad (5)$$

When the spin-flavor quantum numbers are explicitly added, we obtain the total baryon wave function

$$| {}^{2S+1}\dim\{SU_f(3)\}_J [\dim\{SU_{sf}(6)\}, L^P]_{(v_1, v_2); K} \rangle , \quad (6)$$

where  $S$  and  $J$  are the spin and total angular momentum  $\vec{J} = \vec{L} + \vec{S}$ . For example, in this notation the nucleon and delta wave functions are given by

$$| {}^2\mathbf{8}_{1/2} [56, 0^+]_{(0,0);0} \rangle \quad \text{and} \quad | {}^4\mathbf{10}_{3/2} [56, 0^+]_{(0,0);0} \rangle , \quad (7)$$

respectively.

The second ingredient in the calculation is the form of the operator inducing the strong transition. Several forms have been suggested [15]. We use here the simple form [11]

$$\mathcal{H} = \frac{1}{(2\pi)^{3/2}(2k_0)^{1/2}} \sum_{j=1}^3 X_j^M \left[ 2g(\vec{s}_j \cdot \vec{k})e^{-i\vec{k}\cdot\vec{r}_j} + h\vec{s}_j \cdot (\vec{p}_j e^{-i\vec{k}\cdot\vec{r}_j} + e^{-i\vec{k}\cdot\vec{r}_j} \vec{p}_j) \right] , \quad (8)$$

where  $\vec{r}_j$ ,  $\vec{p}_j$  and  $\vec{s}_j$  are the coordinate, momentum and spin of the  $j$ -th constituent, respectively;  $k_0 = E_M = E_B - E_{B'}$  is the meson energy, and  $\vec{k} = \vec{P}_M = \vec{P} - \vec{P}' = k\hat{z}$  denotes the momentum carried by the outgoing meson. Here  $\vec{P} = P_z\hat{z}$  and  $\vec{P}' (= P'_z\hat{z})$  are the momenta of the initial and final baryon. The coefficients  $g$  and  $h$  denote the strength of the two terms in the transition operator of Eq. (8). The flavor operator  $X_j^M$  (to be discussed below) corresponds to the emission of an elementary meson ( $M$ ) by the  $j$ -th constituent:  $q_j \rightarrow q'_j + M$  (see Figure 2).

Using the symmetry of the wave functions for nonstrange baryons (the only case we discuss here), transforming to Jacobi coordinates and integrating over the baryon center of mass coordinate, we find

$$\mathcal{H} = \frac{1}{(2\pi)^{3/2}(2k_0)^{1/2}} 6X_3^M \left[ gks_{3,z}\hat{U} - h s_{3,z}(\hat{T}_z - \frac{1}{6}(P_z + P'_z)\hat{U}) - \frac{1}{2}h(s_{3,+}\hat{T}_- + s_{3,-}\hat{T}_+) \right] , \quad (9)$$

with

$$\begin{aligned} \hat{U} &= e^{ik\sqrt{\frac{2}{3}}\lambda_z} , \\ \hat{T}_m &= \frac{1}{2} \left( \sqrt{\frac{2}{3}} p_{\lambda,m} e^{ik\sqrt{\frac{2}{3}}\lambda_z} + e^{ik\sqrt{\frac{2}{3}}\lambda_z} \sqrt{\frac{2}{3}} p_{\lambda,m} \right) . \end{aligned} \quad (10)$$

By making the replacement,  $\vec{p}_\lambda/m_q \rightarrow -ik_0\vec{\lambda}$  [16], and the mapping onto the algebraic operators,  $\sqrt{2/3}\lambda_m \rightarrow \beta\hat{D}_{\lambda,m}/X_D$  [4, 5], we can write Eq. (10) as

$$\begin{aligned} \hat{U} &= e^{ik\beta\hat{D}_{\lambda,z}/X_D} , \\ \hat{T}_m &= -\frac{im_q k_0 \beta}{2X_D} \left( \hat{D}_{\lambda,m} e^{ik\beta\hat{D}_{\lambda,z}/X_D} + e^{ik\beta\hat{D}_{\lambda,z}/X_D} \hat{D}_{\lambda,m} \right) . \end{aligned} \quad (11)$$

The dipole operator  $\hat{D}_{\lambda,m}$  is a generator of  $U(7)$  and  $X_D$  is its normalization, as discussed in [4, 5]. The calculation of the matrix elements of  $\mathcal{H}$  can be done in configuration space  $(\vec{\rho}, \vec{\lambda})$  or in momentum

space  $(\vec{p}_\rho, \vec{p}_\lambda)$ . The mapping onto the algebraic space of  $U(7)$  is a convenient way to carry out the calculations, much in the same way as the mapping of coordinates and momenta onto creation and annihilation operators in the harmonic oscillator space.

In the collective model the matrix elements of  $\mathcal{H}$  are obtained by folding with the distribution function  $g(\beta)$  of Eq. (4). These collective matrix elements can be expressed in terms of helicity amplitudes. For decays in which the initial baryon has angular momentum  $\vec{J} = \vec{L} + \vec{S}$  and in which the final baryon is either the nucleon or the delta with  $L' = 0$  and thus  $J' = S'$ , the helicity amplitudes are

$$\begin{aligned}
A_\nu(k) &= \int d\beta g(\beta) \langle \alpha', L' = 0, S', J' = S', M'_J = \nu | \mathcal{H} | \alpha, L, S, J, M_J = \nu \rangle \\
&= \frac{1}{(2\pi)^{3/2} (2k_0)^{1/2}} \left[ \langle L, 0, S, \nu | J, \nu \rangle \zeta_0 Z_0(k) + \frac{1}{2} \langle L, 1, S, \nu - 1 | J, \nu \rangle \zeta_+ Z_-(k) \right. \\
&\quad \left. + \frac{1}{2} \langle L, -1, S, \nu + 1 | J, \nu \rangle \zeta_- Z_+(k) \right].
\end{aligned} \tag{12}$$

Here  $\alpha$  denotes the labels that, in addition to  $L, S, J$  and  $\nu$ , are needed to specify the baryon wave function (see Eq. (6)). The coefficients  $\zeta_m$  are the spin-flavor matrix elements of  $X_3^M s_{3,m}$ , to be discussed below, and  $Z_m(k)$  ( $m = 0, \pm$ ) are the radial matrix elements

$$\begin{aligned}
Z_0(k) &= 6 \int d\beta g(\beta) \langle \alpha', L' = M'_L = 0 | gk \hat{U} - h (\hat{T}_z - \frac{1}{6} (P_z + P'_z) \hat{U}) | \alpha, L, M_L = 0 \rangle \\
&= 6 [gk + h \frac{1}{6} (P_z + P'_z)] \mathcal{F}(k) - 6h \mathcal{G}_z(k), \\
Z_\pm(k) &= -6h \int d\beta g(\beta) \langle \alpha', L' = M'_L = 0 | \hat{T}_\pm | \alpha, L, M_L = \mp 1 \rangle \\
&= -6h \mathcal{G}_\pm(k).
\end{aligned} \tag{13}$$

The calculation of the radial matrix elements is identical to that already reported for electromagnetic couplings [4, 5]. Therefore, we do not repeat it here, but only show in Table I the matrix elements  $\mathcal{F}(k)$  and  $\mathcal{G}_m(k)$  of  $\hat{U}$  and  $\hat{T}_m$ , respectively, for the ‘collective’ model with distribution given by Eq. (4). Note that Table I presents the results for an emission process, whereas the corresponding table for the ‘collective’ model in [4, 5] shows the results for an absorption process. For any other model of baryons with the same spin-flavor structure, the corresponding results can be obtained by replacing Table I with the appropriate table (for example, by using harmonic oscillator wave functions as discussed in [4]).

Contrary to the case of electromagnetic couplings where the spin-flavor part is relatively simple, the calculation of the spin-flavor part for strong decays is somewhat more involved. The spin-flavor matrix elements factorize into a spin matrix element of  $s_{3,m}$  between spin wave functions and a flavor matrix element of  $X_3^M$  between flavor wave functions ( $\phi$  and  $\phi'$ ). The calculation of the spin part is straightforward. For the flavor part we take the flavor operators of the form

$$\begin{aligned}
X^{\pi^+} &= -\frac{1}{\sqrt{2}} (\lambda_1 - i \lambda_2), \\
X^{\pi^0} &= \lambda_3, \\
X^{\pi^-} &= \frac{1}{\sqrt{2}} (\lambda_1 + i \lambda_2),
\end{aligned}$$

$$\begin{aligned}
X^{\eta_8} &= \lambda_8 , \\
X^{\eta_1} &= \sqrt{\frac{2}{3}} \mathcal{I} ,
\end{aligned} \tag{14}$$

where  $\lambda_i$  are the Gell-Mann matrices [17] and  $\mathcal{I}$  denotes the unit operator in flavor space. For the pseudoscalar  $\eta$  mesons we introduce a mixing angle  $\theta_P$  between the octet and singlet mesons [17]

$$\begin{aligned}
\eta &= \eta_8 \cos \theta_P - \eta_1 \sin \theta_P , \\
\eta' &= \eta_8 \sin \theta_P + \eta_1 \cos \theta_P ,
\end{aligned} \tag{15}$$

and similarly for the corresponding flavor operators

$$\begin{aligned}
X^\eta &= X^{\eta_8} \cos \theta_P - X^{\eta_1} \sin \theta_P , \\
X^{\eta'} &= X^{\eta_8} \sin \theta_P + X^{\eta_1} \cos \theta_P .
\end{aligned} \tag{16}$$

The flavor operators  $X_3^M$  appearing in Eq. (9) only act on the 3-rd constituent. The corresponding matrix elements can either be evaluated explicitly for each channel separately, or more conveniently, by using the Wigner-Eckart theorem and isoscalar factors of  $SU_f(3)$  [18]. For the decay process  $B \rightarrow B' + M$  we have

$$\begin{aligned}
\langle \phi' | X_3^M | \phi \rangle &= \langle (p_2, q_2), I_2, M_{I_2}, Y_2 | T^{(p,q), I, M_I, Y} | (p_1, q_1), I_1, M_{I_1}, Y_1 \rangle \\
&= \langle I_1, M_{I_1}, I, M_I | I_2, M_{I_2} \rangle \sum_\gamma \left\langle \begin{array}{cc} (p_1, q_1) & (p, q) \\ I_1, Y_1 & I, Y \end{array} \middle| \begin{array}{c} (p_2, q_2)_\gamma \\ I_2, Y_2 \end{array} \right\rangle \\
&\quad \times \langle (p_2, q_2) || T^{(p,q)} || (p_1, q_1) \rangle_\gamma .
\end{aligned} \tag{17}$$

In this notation  $(p_i, q_i) = (1, 1)$  or  $(3, 0)$  for the baryon flavor octet and decuplet, respectively, and  $(p, q) = (1, 1)$  or  $(0, 0)$  for the meson flavor octet and singlet, respectively (see Eq. (14)). The sum over  $\gamma$  is over different multiplicities. The flavor states are labeled by the quantum numbers  $(p, q), I, M_I, Y$  corresponding to the reduction  $SU_f(3) \supset SU_I(2) \otimes U_Y(1)$ . The right hand side contains the sum of products of an isospin Clebsch-Gordan coefficient, which contains the dependence on the charge channel, a  $SU(3)$  isoscalar factor, which depends on the isospin channel, and a  $SU(3)$  reduced matrix element, which depends on the coupling of the flavor multiplets  $(p, q)$ , but not on isospin  $I, M_I$  and hypercharge  $Y$ . In Table II we give the expressions for the  $SU_f(3)$  reduced matrix elements.

Using Eqs. (14)–(17) and the matrix elements of the spin operator, we can compute all spin-flavor matrix elements for a given isospin channel. In Tables III and IV we present the results for the decay into  $\pi$  and  $\eta, \eta'$ , respectively. Results for a specific charge channel can be obtained by multiplying with the appropriate isospin Clebsch-Gordan coefficient.

The helicity amplitudes  $A_\nu(k)$  of Eq. (12) can be converted to partial wave amplitudes  $a_l(k)$  by [19]

$$\begin{aligned}
A_\nu(k) &= \sum_{l=L\pm 1} \sqrt{2l+1} \langle l, 0, J', \nu | J, \nu \rangle a_l(k) , \\
a_l(k) &= \frac{1}{2J+1} \sum_\nu \sqrt{2l+1} \langle l, 0, J', \nu | J, \nu \rangle A_\nu(k) .
\end{aligned} \tag{18}$$

Here  $l$  is the relative orbital angular momentum between the final baryon and the emitted meson. It takes the values  $l = L \pm 1$  (the value  $l = L$  is not allowed because of parity conservation). With the definition of the transition operator in Eq. (8) and the helicity amplitudes and partial wave amplitudes, the decay widths for a specific isospin channel are given by [15]

$$\begin{aligned}\Gamma(B \rightarrow B' + M) &= 2\pi\rho_f \frac{2}{2J+1} \sum_{\nu>0} |A_\nu(k)|^2 \\ &= 2\pi\rho_f \sum_{l=L\pm 1} |a_l(k)|^2 ,\end{aligned}\tag{19}$$

where  $\rho_f$  is a phase space factor for the final state which depends on the choice of the reference frame.

### III Results

For all resonances with the same value of  $(v_1, v_2)$ ,  $L^P$  the expression for the decay widths of Eq. (19) can be rewritten in a more transparent form in terms of only two elementary partial wave amplitudes  $W_l(k)$ ,

$$\Gamma(B \rightarrow B' + M) = 2\pi\rho_f \sum_{l=L\pm 1} |a_l(k)|^2 = 2\pi\rho_f \frac{1}{(2\pi)^3 2k_0} \sum_{l=L\pm 1} c_l |W_l(k)|^2 .\tag{20}$$

For this set of resonances, the  $k$  dependence of the partial wave amplitudes  $a_l(k)$  is contained in the amplitudes  $W_l(k)$ , while the dependence on the individual baryon resonance is contained in the coefficients  $c_l$ . In the algebraic method, the elementary partial wave amplitudes  $W_l(k)$  can be obtained in closed form.

In Table V we present the values of  $c_l$  for the negative parity resonances with  $(v_1, v_2)$ ,  $L^P = (0, 0), 1^-$ . In the ‘collective’ model with distribution given by Eq. (4) the corresponding  $S$  and  $D$  elementary partial wave amplitudes are

$$\begin{aligned}W_0(k) &= i \left\{ [gk + \frac{1}{6}h(P_z + P'_z)] \frac{ka}{(1+k^2a^2)^2} + h m_3 k_0 a \frac{3-k^2a^2}{(1+k^2a^2)^3} \right\} , \\ W_2(k) &= i \left\{ [gk + \frac{1}{6}h(P_z + P'_z)] \frac{ka}{(1+k^2a^2)^2} - h m_3 k_0 a \frac{4k^2a^2}{(1+k^2a^2)^3} \right\} .\end{aligned}\tag{21}$$

Similarly, in Table VI we present the  $c_l$  coefficients for the positive parity resonances with  $(v_1, v_2)$ ,  $L^P = (0, 0), 2^+$ . The corresponding  $P$  and  $F$  elementary partial wave amplitudes are

$$\begin{aligned}W_1(k) &= [gk + \frac{1}{6}h(P_z + P'_z)] \left\{ \frac{-1}{(1+k^2a^2)^2} + \frac{3}{2k^3a^3} H(ka) \right\} \\ &\quad + h m_3 k_0 a \frac{1}{ka} \frac{4k^2a^2}{(1+k^2a^2)^3} , \\ W_3(k) &= [gk + \frac{1}{6}h(P_z + P'_z)] \left\{ \frac{-1}{(1+k^2a^2)^2} + \frac{3}{2k^3a^3} H(ka) \right\} \\ &\quad + h m_3 k_0 a \frac{1}{ka} \left\{ \frac{5+9k^2a^2}{(1+k^2a^2)^3} - \frac{15}{2k^3a^3} H(ka) \right\} ,\end{aligned}\tag{22}$$

with  $H(ka) = \arctan ka - ka/(1+k^2a^2)$ . The sum of the momenta of the initial and final resonance,  $P_z + P'_z$ , appearing in Eqs. (21) and (22) depends on the choice of the reference frame.

Partial widths for other models of the nucleon and its resonances can be obtained by introducing the corresponding expressions for the elementary amplitudes  $W_l(k)$ . For example, the relevant expressions in the harmonic oscillator quark model are

$$\begin{aligned} W_0(k) &= \frac{i}{3} \left\{ [gk + \frac{1}{6}h(P_z + P'_z)]k\beta + hm_3k_0\beta(3 - \frac{k^2\beta^2}{3}) \right\} e^{-k^2\beta^2/6}, \\ W_2(k) &= \frac{i}{3} \left\{ [gk + \frac{1}{6}h(P_z + P'_z)]k\beta - \frac{1}{3}hm_3k_0\beta k^2\beta^2 \right\} e^{-k^2\beta^2/6}, \end{aligned} \quad (23)$$

and

$$\begin{aligned} W_1(k) &= \frac{\sqrt{2}}{3\sqrt{15}}k\beta \left\{ [gk + \frac{1}{6}h(P_z + P'_z)]k\beta + hm_3k_0\beta(5 - \frac{k^2\beta^2}{3}) \right\} e^{-k^2\beta^2/6}, \\ W_3(k) &= \frac{\sqrt{2}}{3\sqrt{15}}k\beta \left\{ [gk + \frac{1}{6}h(P_z + P'_z)]k\beta - \frac{1}{3}hm_3k_0\beta k^2\beta^2 \right\} e^{-k^2\beta^2/6}. \end{aligned} \quad (24)$$

## IV Analysis of experimental data

Use of Eqs. (20)–(22) allows us to do a straightforward and systematic analysis of the experimental data. These expressions contain the external momenta, and hence depend on the choice of reference frame. This leads to ambiguities in comparing with data. Here we adopt the procedure of [15], in which calculations are performed in the rest frame of the decaying resonance, and in which the relativistic expression for the phase space factor  $\rho_f$  as well as for the momentum  $k$  of the emitted meson are retained. In this frame of reference  $P_z = 0$  and hence  $P'_z = -k$ . The expressions for  $k$  and  $\rho_f$  are

$$\begin{aligned} k^2 &= -m_M^2 + \frac{(m_B^2 - m_{B'}^2 + m_M^2)^2}{4m_B^2}, \\ \rho_f &= \int d\vec{P}' d\vec{P}_M \delta(m_B - E_{B'}(P_M) - E_M(P_M)) \delta(\vec{P}' + \vec{P}_M) \\ &= 4\pi \frac{E_{B'}(k)E_M(k)k}{m_B} \end{aligned} \quad (25)$$

with  $E_{B'}(k) = \sqrt{m_{B'}^2 + k^2}$  and  $E_M(k) = \sqrt{m_M^2 + k^2}$ .

We consider here decays with emission of  $\pi$  and  $\eta$ . The experimental data, extracted from the compilation by the Particle Data Group [17] are shown in Tables VII, VIII and IX, where they are compared with the results of our calculation. The calculated values depend on the two parameters  $g$  and  $h$  in the transition operator of Eq. (8), and on the scale parameter  $a$  of Eq. (4). We keep  $g$ ,  $h$  and  $a$  equal for *all* resonances and *all* decay channels ( $N\pi$ ,  $N\eta$ ,  $\Delta\pi$ ,  $\Delta\eta$ ). In comparing with previous calculations, it should be noted that in the calculation in the nonrelativistic quark model of [11] the decay widths are parametrized by four reduced partial wave amplitudes instead of the two elementary amplitudes  $g$  and  $h$ . Furthermore, the momentum dependence of these reduced amplitudes are represented by constants. The calculation in the relativized quark model of [12] was done using a pair-creation model for the decay and involved a different assumption on the phase space factor. Both the nonrelativistic and relativized



quark model calculations include the effects of mixing induced by the hyperfine interaction, which in the present calculation are not taken into account.

In the present analysis we determine the values of  $g$ ,  $h$  and  $a$  from a least square fit to the  $N\pi$  partial widths (which are relatively well known) with the exclusion of the  $S_{11}$  resonances. For the latter the situation is not clear due to possible mixing of  $N(1535)S_{11}$  and  $N(1650)S_{11}$  and the possible existence of a third  $S_{11}$  resonance [9]. As a result we find  $g = 1.164 \text{ GeV}^{-1}$  and  $h = -0.094 \text{ GeV}^{-1}$ . The relative sign is consistent with a previous analysis of the strong decay of mesons [20] and with a derivation from the axial-vector coupling (see *e.g.* [15]). The scale parameter,  $a = 0.232 \text{ fm}$ , extracted in the present fit is found to be equal to the value extracted in the calculation of electromagnetic couplings [5]. Just as in our study of the electromagnetic couplings [5] we present the strong decays of the resonances, that in the ‘collective’ model are assigned as vibrational excitations of the configuration of Fig. 1, in terms of two coefficients,  $\chi_1 = (1 - R^2)/R\sqrt{N}$  and  $\chi_2 = \sqrt{1 + R^2}/R\sqrt{N}$ , one for each fundamental vibration (here  $N$  determines the size of the model space and  $R^2$  is a size parameter, as discussed in [4]).

The calculation of decay widths into the  $N\pi$  channel, as shown for the 3 and 4 star resonances in Table VII, is in fair agreement with experiment. This is emphasized in Figs. 3 and 4. The results are to a large extent a consequence of spin-flavor symmetry. The use of ‘collective’ form factors improves somewhat the results when compared with older (harmonic oscillator) calculations. This is shown in Table X where the decay of a  $\Delta$  Regge trajectory into  $N\pi$  is analyzed and compared with the calculations of [15], which are based on the harmonic oscillator model discussed in [21]. We also include the results of more recent calculations in the nonrelativistic quark model [11] and in the relativized quark model [12]. There does not seem to be anything unusual in the decays into  $\pi$  and our analysis confirms the results of previous analyses. In Table XI we show the  $N\pi$  decays of the calculated resonances below 2 GeV which have not been observed (missing resonances). The resonances with  $L^P = 1^+$  and  $L^P = 2^-$  are decoupled because of the spin-flavor symmetry. Most of other resonances have small decay widths, with the exception of the  $P_{13}$  and  $F_{15}$  states, which have widths comparable to those of the well-established  $P_{13}$  and  $F_{15}$  states of Table VII. This behaviour can be understood by inspection of Table VI. The coefficients for the  $P_{13}$  states are  $c_1 = 25/12$  and  $c_1 = 2$ . This leads to comparable  $N\pi$  widths of 31 MeV and 56 MeV, respectively. The difference is due to the  $k$  values of these resonances that enter in the elementary partial wave amplitude  $W_1(k)$  of Eq. (22). A similar situation holds for the  $F_{15}$  states. The relative magnitude of the  $c_l$  coefficients in Table VI explain the smaller decay widths for the other missing resonances of Table XI.

Contrary to the decays into  $\pi$ , the decay widths into  $\eta$  have some unusual properties. The calculation gives systematically small values for these widths. This is due to a combination of phase space factors and the structure of the transition operator. Both depend on the momentum transfer  $k$ . The values of  $k$  in Tables VII, VIII and IX show that, due to the difference between the  $\pi$  and  $\eta$  mass, the momentum carried by the  $\eta$  is smaller than that carried by the  $\pi$ . Therefore, the  $\eta$  decay widths are suppressed relative to the  $\pi$  decays. The spin-flavor part is approximately the same for  $N\pi$  and  $N\eta$ , since  $\pi$  and  $\eta$

are in the same  $SU_f(3)$  multiplet. We emphasize here, that the transition operator was determined by fitting the coefficients  $g$  and  $h$  to the  $N\pi$  decays of the 3 and 4 star resonances. Hence the  $\eta$  decays are calculated without introducing any further parameters.

The experimental situation is unclear. The 1992 PDG compilation [22] gave systematically small widths ( $\sim 1$  MeV) for all resonances except  $N(1535)S_{11}$ . The 1994 PDG compilation [23] deleted all  $\eta$  widths with the exception of  $N(1535)S_{11}$ . This situation persists in the latest PDG compilation [17], where  $N(1650)S_{11}$  is now assigned a small but non-zero  $\eta$  width. The results of our analysis suggest that the large  $\eta$  width for the  $N(1535)S_{11}$  is not due to a conventional  $q^3$  state. One possible explanation is the presence of another state in the same mass region, *e.g.* a quasi-bound meson-baryon  $S$  wave resonance, just below or above threshold. Recently it was suggested [8] that a quasi-bound  $K\Sigma$ - $K\Lambda$  state with properties remarkably similar to the  $N(1535)S_{11}$  resonance could be responsible for the large  $N\eta$  branch of the  $N(1535)S_{11}$  resonance.

For possible use in the analysis of new experimental data, we give in Table XI the strong decay widths of the so-called missing resonances with a calculated mass below 2 GeV which up to now have not been observed experimentally.

## V Conclusions

We have presented a calculation of the strong decay widths  $N^* \rightarrow N + \pi$ ,  $N^* \rightarrow \Delta + \pi$ ,  $N^* \rightarrow N + \eta$ ,  $\Delta^* \rightarrow N + \pi$ ,  $\Delta^* \rightarrow \Delta + \pi$  and  $\Delta^* \rightarrow \Delta + \eta$  in a collective model of baryons. By exploiting the symmetry of the problem, both in its spin-flavor-color part,  $SU_{sf}(6) \otimes SU_c(3)$ , and in its space part,  $U(7)$ , we have been able to write the results in a transparent analytic way (Section III). The analysis of experimental data shows that, while the decays into  $\pi$  follow the expected pattern, the decays into  $\eta$  have some unusual features. Our calculations do not show any indication for a large  $\eta$  width, as is observed for the  $N(1535)S_{11}$  resonance. The observed large  $\eta$  width indicates the presence of another configuration, which is outside the present model space. A possible candidate for such a configuration is a quasi-bound meson-baryon  $S$  wave resonance ( $K\Sigma - K\Lambda$ ) [8]. This suggests, that in order to elucidate this point, particular attention be paid at CEBAF to the  $N\eta$  channel.

Our calculations can be easily extended to include other decay channels, such as  $\Lambda K$  and  $\Sigma K$ . These calculations are currently underway and are part of the extension of the model to include strange resonances as well.

## Acknowledgements

We wish to thank T.-S. H. Lee and D. Kurath for interesting discussions. This work is supported in part by CONACyT, México under project 400340-5-3401E, DGAPA-UNAM under project IN105194 (R.B.), by D.O.E. Grant DE-FG02-91ER40608 (F.I.) and by grant No. 94-00059 from the United States-Israel

Binational Science Foundation (BSF), Jerusalem, Israel (A.L.).

## References

- [1] M. Gell-Mann, Phys. Rev. **125**, 1067 (1962).
- [2] Y. Ne'eman, Nucl. Phys. **26**, 222 (1961).
- [3] F. Gürsey and L.A. Radicati, Phys. Rev. Lett. **13**, 173 (1964).
- [4] R. Bijker, F. Iachello and A. Leviatan, Ann. Phys. (N.Y.) **236**, 69 (1994).
- [5] R. Bijker, F. Iachello and A. Leviatan, preprint nucl-th/9510001, Phys. Rev. C, in press.
- [6] M. Benmerrouche and N.C. Mukhopadhyay, Phys. Rev. Lett. **67**, 1070 (1991); M. Benmerrouche, N.C. Mukhopadhyay and J.F. Zhang, Phys. Rev. **D51**, 3237 (1995); N.C. Mukhopadhyay, J.F. Zhang and M. Benmerrouche, Phys. Lett. **B364**, 1 (1995).
- [7] Z. Li, Phys. Rev. **D52**, 4961 (1995).
- [8] N. Kaiser, P.B. Siegel and W. Weise, Phys. Lett. **B362**, 23 (1995).
- [9] Z. Li and R. Workman, Phys. Rev. **C53**, R549 (1996).
- [10] L.Ya. Glozman and D.O. Riska, Phys. Lett. **B366**, 305 (1996).
- [11] R. Koniuk and N. Isgur, Phys. Rev. Lett. **44**, 845 (1980); Phys. Rev. **D21**, 1868 (1980).
- [12] S. Capstick and W. Roberts, Phys. Rev. **D47**, 1994 (1993); *ibid.* **D49**, 4570 (1994).
- [13] N. Isgur and G. Karl, Phys. Rev. **D18**, 4187 (1978); **D19**, 2653 (1979); **D20**, 1191 (1979).
- [14] S. Capstick and N. Isgur, Phys. Rev. **D34**, 2809 (1986).
- [15] A. Le Yaouanc, L. Oliver, O. Pène and J.-C. Raynal, 'Hadron transitions in the quark model', Gordon and Breach (1988).
- [16] R. McClary and N. Byers, Phys. Rev. **D28**, 1692 (1983).
- [17] Particle Data Group, Phys. Rev. **D54**, 1 (1996).
- [18] J.J. de Swart, Rev. Mod. Phys. **35**, 916 (1963).
- [19] W.P. Petersen and J.L. Rosner, Phys. Rev. **D6**, 820 (1972).
- [20] C. Gobbi, F. Iachello and D. Kusnezov, Phys. Rev. **D50**, 2048 (1994).
- [21] R.H. Dalitz, in 'Quarks and Hadronic Structure', Ed. M. Morpurgo, Plenum (1977).
- [22] Particle Data Group, Phys. Rev. **D45**, S1 (1992).
- [23] Particle Data Group, Phys. Rev. **D50**, 1173 (1994).

Table I: Matrix elements  $\mathcal{F}(k)$  and  $\mathcal{G}(k)$  in the collective model for  $N \rightarrow \infty$  (large model space). The final state is  $[56, 0^+]_{(0,0);0}$ . The matrix elements for the vibrational excitations are given in terms of  $\chi_1 = (1 - R^2)/R\sqrt{N}$  and  $\chi_2 = \sqrt{1 + R^2}/R\sqrt{N}$  [4, 5].  $H(x) = \arctan x - x/(1 + x^2)$ .

Initial state	$\mathcal{F}(k)$	$\mathcal{G}_z(k)/m_3 k_0 a$	$\mathcal{G}_\pm(k)/m_3 k_0 a$
$[56, 0^+]_{(0,0);0}$	$\frac{1}{(1+k^2 a^2)^2}$	$\frac{4ka}{(1+k^2 a^2)^3}$	0
$[20, 1^+]_{(0,0);0}$	0	0	0
$[70, 1^-]_{(0,0);1}$	$i\sqrt{3} \frac{ka}{(1+k^2 a^2)^2}$	$-i\sqrt{3} \frac{1-3k^2 a^2}{(1+k^2 a^2)^3}$	$\mp i\sqrt{6} \frac{1}{(1+k^2 a^2)^2}$
$[56, 2^+]_{(0,0);0}$	$\frac{1}{2}\sqrt{5} \left[ \frac{-1}{(1+k^2 a^2)^2} + \frac{3}{2k^3 a^3} H(ka) \right]$	$-\frac{1}{2}\sqrt{5} \left[ \frac{3+7k^2 a^2}{ka(1+k^2 a^2)^3} - \frac{9}{2k^4 a^4} H(ka) \right]$	$\mp \sqrt{\frac{15}{2}} \left[ \frac{-1}{ka(1+k^2 a^2)^2} + \frac{3}{2k^4 a^4} H(ka) \right]$
$[70, 2^-]_{(0,0);1}$	0	0	0
$[70, 2^+]_{(0,0);2}$	$-\frac{1}{2}\sqrt{15} \left[ \frac{-1}{(1+k^2 a^2)^2} + \frac{3}{2k^3 a^3} H(ka) \right]$	$\frac{1}{2}\sqrt{15} \left[ \frac{3+7k^2 a^2}{ka(1+k^2 a^2)^3} - \frac{9}{2k^4 a^4} H(ka) \right]$	$\pm \frac{3}{2}\sqrt{10} \left[ \frac{-1}{ka(1+k^2 a^2)^2} + \frac{3}{2k^4 a^4} H(ka) \right]$
$[56, 0^+]_{(1,0);0}$	$-\chi_1 \frac{2k^2 a^2}{(1+k^2 a^2)^3}$	$\chi_1 \frac{4ka(1-2k^2 a^2)}{(1+k^2 a^2)^4}$	0
$[70, 1^-]_{(1,0);1}$	$i\frac{1}{2}\sqrt{3} \chi_1 \frac{ka(1-3k^2 a^2)}{(1+k^2 a^2)^3}$	$-i\frac{1}{2}\sqrt{3} \chi_1 \frac{1-14k^2 a^2+9k^4 a^4}{(1+k^2 a^2)^4}$	$\mp i\sqrt{\frac{3}{2}} \chi_1 \frac{1-3k^2 a^2}{(1+k^2 a^2)^3}$
$[70, 0^+]_{(0,1);0}$	$\chi_2 \frac{2k^2 a^2}{(1+k^2 a^2)^3}$	$-\chi_2 \frac{4ka(1-2k^2 a^2)}{(1+k^2 a^2)^4}$	0
$[70, 1^-]_{(0,1);1}$	$-i\sqrt{\frac{3}{2}} \chi_2 \frac{ka(1-k^2 a^2)}{(1+k^2 a^2)^3}$	$i\sqrt{\frac{3}{2}} \chi_2 \frac{1-8k^2 a^2+3k^4 a^4}{(1+k^2 a^2)^4}$	$\pm i\sqrt{3} \chi_2 \frac{1-k^2 a^2}{(1+k^2 a^2)^3}$
$[56, 1^-]_{(0,1);1}$	$-i\sqrt{6} \chi_2 \frac{k^3 a^3}{(1+k^2 a^2)^3}$	$i\sqrt{6} \chi_2 \frac{3k^2 a^2(1-k^2 a^2)}{(1+k^2 a^2)^4}$	$\pm i2\sqrt{3} \chi_2 \frac{k^2 a^2}{(1+k^2 a^2)^3}$

Table II:  $SU_f(3)$  reduced matrix elements.

		$\langle (p_2, q_2)    T^{(1,1)}    (p_1, q_1) \rangle_\gamma$	
$(p_2, q_2)$	$(p_1, q_1)$	$\gamma = 1$	$\gamma = 2$
$(1, 1)_\lambda$	$(1, 1)_\lambda$	$-\frac{\sqrt{5}}{\sqrt{3}}$	$\frac{1}{\sqrt{3}}$
$(1, 1)_\rho$	$(1, 1)_\rho$	$\frac{\sqrt{5}}{\sqrt{3}}$	$\sqrt{3}$
$(3, 0)$	$(3, 0)$	$\frac{2\sqrt{2}}{\sqrt{3}}$	
$(3, 0)$	$(1, 1)_\lambda$	$\frac{2\sqrt{2}}{\sqrt{3}}$	
$(3, 0)$	$(1, 1)_\rho$	0	
$(1, 1)_\lambda$	$(3, 0)$	$-\frac{\sqrt{10}}{\sqrt{3}}$	
$(1, 1)_\rho$	$(3, 0)$	0	

Table III: Spin-flavor matrix elements  $\zeta_m$  ( $m = 0, \pm$ ) of Eq. (12) for strong decay of baryons  $B \rightarrow B' + M$  with  $M = \pi$ . The final state is  ${}^2 8_{1/2}[56, 0^+]$  for the nucleon ( $B' = N$ ) and  ${}^4 10_{3/2}[56, 0^+]$  for the delta ( $B' = \Delta$ ).

Initial State	$A_{1/2}(N\pi)$			$A_{1/2}(\Delta\pi)$			$A_{3/2}(\Delta\pi)$		
	$\zeta_0$	$\zeta_+$	$\zeta_-$	$\zeta_0$	$\zeta_+$	$\zeta_-$	$\zeta_0$	$\zeta_+$	$\zeta_-$
${}^2 8_J[56, L^P]$	$\frac{5}{6\sqrt{3}}$	$\frac{5}{3\sqrt{3}}$	0	$\frac{-2\sqrt{2}}{3\sqrt{3}}$	$\frac{2\sqrt{2}}{3\sqrt{3}}$	0	0	$\frac{2\sqrt{2}}{3}$	0
${}^2 8_J[70, L^P]$	$\frac{\sqrt{2}}{3\sqrt{3}}$	$\frac{2\sqrt{2}}{3\sqrt{3}}$	0	$\frac{2}{3\sqrt{3}}$	$\frac{-2}{3\sqrt{3}}$	0	0	$\frac{-2}{3}$	0
${}^4 8_J[70, L^P]$	$\frac{1}{3\sqrt{6}}$	$\frac{1}{3\sqrt{6}}$	$\frac{-1}{3\sqrt{2}}$	$\frac{1}{3\sqrt{3}}$	$\frac{4}{3\sqrt{3}}$	$\frac{2}{3}$	$\frac{1}{\sqrt{3}}$	$\frac{2}{3}$	0
${}^2 8_J[20, L^P]$	0	0	0	0	0	0	0	0	0
${}^4 10_J[56, L^P]$	$\frac{2}{3\sqrt{3}}$	$\frac{2}{3\sqrt{3}}$	$\frac{-2}{3}$	$\frac{\sqrt{5}}{6\sqrt{3}}$	$\frac{2\sqrt{5}}{3\sqrt{3}}$	$\frac{\sqrt{5}}{3}$	$\frac{\sqrt{5}}{2\sqrt{3}}$	$\frac{\sqrt{5}}{3}$	0
${}^2 10_J[70, L^P]$	$\frac{1}{6\sqrt{3}}$	$\frac{1}{3\sqrt{3}}$	0	$\frac{-\sqrt{5}}{3\sqrt{3}}$	$\frac{\sqrt{5}}{3\sqrt{3}}$	0	0	$\frac{\sqrt{5}}{3}$	0

Table IV: Same as Table III, but with  $M = \eta$  and  $M = \eta'$  corresponding to  $\xi = (\cos \theta_P - \sqrt{2} \sin \theta_P)/\sqrt{3}$  and  $\xi = (\sin \theta_P + \sqrt{2} \cos \theta_P)/\sqrt{3}$ , respectively.

Initial State	$A_{1/2}(N\eta)/\xi$			$A_{1/2}(\Delta\eta)/\xi$			$A_{3/2}(\Delta\eta)/\xi$		
	$\zeta_0$	$\zeta_+$	$\zeta_-$	$\zeta_0$	$\zeta_+$	$\zeta_-$	$\zeta_0$	$\zeta_+$	$\zeta_-$
${}^2 8_J[56, L^P]$	$\frac{1}{6}$	$\frac{1}{3}$	0	0	0	0	0	0	0
${}^2 8_J[70, L^P]$	$\frac{1}{3\sqrt{2}}$	$\frac{\sqrt{2}}{3}$	0	0	0	0	0	0	0
${}^4 8_J[70, L^P]$	$\frac{-1}{3\sqrt{2}}$	$\frac{-1}{3\sqrt{2}}$	$\frac{1}{\sqrt{6}}$	0	0	0	0	0	0
${}^2 8_J[20, L^P]$	0	0	0	0	0	0	0	0	0
${}^4 10_J[56, L^P]$	0	0	0	$\frac{1}{6}$	$\frac{2}{3}$	$\frac{1}{\sqrt{3}}$	$\frac{1}{2}$	$\frac{1}{\sqrt{3}}$	0
${}^2 10_J[70, L^P]$	0	0	0	$\frac{-1}{3}$	$\frac{1}{3}$	0	0	$\frac{1}{\sqrt{3}}$	0



Table V: Coefficients  $c_i$  of Eq. (20) for the strong decay widths  $B \rightarrow B' + M$  of the negative parity resonances with  $(v_1, v_2), L^P = (0, 0), 1^-$ . The final state is  ${}^2\mathbf{8}_{1/2}[56, 0^+]_{(0,0);0}$  for the nucleon ( $B' = N$ ) and  ${}^4\mathbf{10}_{3/2}[56, 0^+]_{(0,0);0}$  for the delta ( $B' = \Delta$ ).  $\xi$  is defined in the caption of Table IV.

State		$N\pi$		$N\eta$		$\Delta\pi$		$\Delta\eta$	
		$c_0$	$c_2$	$c_0$	$c_2$	$c_0$	$c_2$	$c_0$	$c_2$
$S_{11}$	${}^2\mathbf{8}_{1/2}[70, 1^-]_{(0,0);1}$	$\frac{8}{3}$		$2\xi^2$			$\frac{16}{3}$		
$D_{13}$	${}^2\mathbf{8}_{3/2}[70, 1^-]_{(0,0);1}$		$\frac{8}{3}$		$2\xi^2$	$\frac{8}{3}$	$\frac{8}{3}$		
$S_{11}$	${}^4\mathbf{8}_{1/2}[70, 1^-]_{(0,0);1}$	$\frac{2}{3}$		$2\xi^2$			$\frac{4}{3}$		
$D_{13}$	${}^4\mathbf{8}_{3/2}[70, 1^-]_{(0,0);1}$		$\frac{1}{15}$		$\frac{1}{5}\xi^2$	$\frac{20}{3}$	$\frac{64}{15}$		
$D_{15}$	${}^4\mathbf{8}_{5/2}[70, 1^-]_{(0,0);1}$		$\frac{2}{5}$		$\frac{6}{5}\xi^2$		$\frac{28}{5}$		
$S_{31}$	${}^2\mathbf{10}_{1/2}[70, 1^-]_{(0,0);1}$	$\frac{1}{3}$					$\frac{20}{3}$		$4\xi^2$
$D_{33}$	${}^2\mathbf{10}_{3/2}[70, 1^-]_{(0,0);1}$		$\frac{1}{3}$			$\frac{10}{3}$	$\frac{10}{3}$	$2\xi^2$	$2\xi^2$

Table VI: Coefficients  $c_i$  of Eq. (20) for the strong decay widths of the positive parity resonances with  $(v_1, v_2), L^P = (0, 0), 2^+$ . For notation see Table V.

State	$N\pi$		$N\eta$		$\Delta\pi$		$\Delta\eta$	
	$c_1$	$c_3$	$c_1$	$c_3$	$c_1$	$c_3$	$c_1$	$c_3$
$P_{13}$ ${}^2 8_{3/2}[56, 2^+]_{(0,0);0}$	$\frac{25}{12}$		$\frac{1}{4}\xi^2$		$\frac{4}{15}$	$\frac{12}{5}$		
$F_{15}$ ${}^2 8_{5/2}[56, 2^+]_{(0,0);0}$		$\frac{25}{12}$	$\frac{1}{4}\xi^2$		$\frac{8}{5}$	$\frac{16}{15}$		
$P_{13}$ ${}^2 8_{3/2}[70, 2^+]_{(0,0);2}$	2		$\frac{3}{2}\xi^2$		$\frac{2}{5}$	$\frac{18}{5}$		
$F_{15}$ ${}^2 8_{5/2}[70, 2^+]_{(0,0);2}$		2	$\frac{3}{2}\xi^2$		$\frac{12}{5}$	$\frac{8}{5}$		
$P_{11}$ ${}^4 8_{1/2}[70, 2^+]_{(0,0);2}$	$\frac{1}{2}$		$\frac{3}{2}\xi^2$		1			
$P_{13}$ ${}^4 8_{3/2}[70, 2^+]_{(0,0);2}$	$\frac{1}{4}$		$\frac{3}{4}\xi^2$		$\frac{16}{5}$	$\frac{9}{5}$		
$F_{15}$ ${}^4 8_{5/2}[70, 2^+]_{(0,0);2}$		$\frac{1}{14}$	$\frac{3}{14}\xi^2$		$\frac{21}{5}$	$\frac{128}{35}$		
$F_{17}$ ${}^4 8_{7/2}[70, 2^+]_{(0,0);2}$		$\frac{9}{28}$	$\frac{27}{28}\xi^2$			$\frac{27}{7}$		
$P_{31}$ ${}^4 10_{1/2}[56, 2^+]_{(0,0);0}$	$\frac{4}{3}$				$\frac{5}{12}$		$\frac{1}{4}\xi^2$	
$P_{33}$ ${}^4 10_{3/2}[56, 2^+]_{(0,0);0}$	$\frac{2}{3}$				$\frac{4}{3}$	$\frac{3}{4}$	$\frac{4}{5}\xi^2$	$\frac{9}{20}\xi^2$
$F_{35}$ ${}^4 10_{5/2}[56, 2^+]_{(0,0);0}$		$\frac{4}{21}$			$\frac{7}{4}$	$\frac{32}{21}$	$\frac{21}{20}\xi^2$	$\frac{32}{35}\xi^2$
$F_{37}$ ${}^4 10_{7/2}[56, 2^+]_{(0,0);0}$		$\frac{6}{7}$				$\frac{45}{28}$		$\frac{27}{28}\xi^2$
$P_{33}$ ${}^2 10_{3/2}[70, 2^+]_{(0,0);2}$	$\frac{1}{4}$				$\frac{1}{2}$	$\frac{9}{2}$	$\frac{3}{10}\xi^2$	$\frac{27}{10}\xi^2$
$F_{35}$ ${}^2 10_{5/2}[70, 2^+]_{(0,0);2}$		$\frac{1}{4}$			3	2	$\frac{9}{5}\xi^2$	$\frac{6}{5}\xi^2$

Table VII:  $N\pi$  decay widths of (3 and 4 star) nucleon and delta resonances in MeV. The experimental values are taken from [17]. The mixing angle for the  $\eta$  mesons is  $\theta_P = -23^\circ$  [20].  $\chi_1$  and  $\chi_2$  are defined in the caption of Table I.

State	Mass	Resonance	$k(\text{MeV})$	$\Gamma(\text{th})$	$\Gamma(\text{exp})$
$S_{11}$	$N(1535)$	$^2 8_{1/2}[70, 1^-]_{(0,0);1}$	467	85	$79 \pm 38$
$S_{11}$	$N(1650)$	$^4 8_{1/2}[70, 1^-]_{(0,0);1}$	547	35	$130 \pm 27$
$P_{13}$	$N(1720)$	$^2 8_{3/2}[56, 2^+]_{(0,0);0}$	594	31	$22 \pm 11$
$D_{13}$	$N(1520)$	$^2 8_{3/2}[70, 1^-]_{(0,0);1}$	456	115	$67 \pm 9$
$D_{13}$	$N(1700)$	$^4 8_{3/2}[70, 1^-]_{(0,0);1}$	580	5	$10 \pm 7$
$D_{15}$	$N(1675)$	$^4 8_{5/2}[70, 1^-]_{(0,0);1}$	564	31	$72 \pm 12$
$F_{15}$	$N(1680)$	$^2 8_{5/2}[56, 2^+]_{(0,0);0}$	567	41	$84 \pm 9$
$G_{17}$	$N(2190)$	$^2 8_{7/2}[70, 3^-]_{(0,0);1}$	888	34	$67 \pm 27$
$G_{19}$	$N(2250)$	$^4 8_{9/2}[70, 3^-]_{(0,0);1}$	923	7	$38 \pm 21$
$H_{19}$	$N(2220)$	$^2 8_{9/2}[56, 4^+]_{(0,0);0}$	905	15	$65 \pm 28$
$I_{1,11}$	$N(2600)$	$^2 8_{11/2}[70, 5^-]_{(0,0);1}$	1126	9	$49 \pm 20$
$P_{11}$	$N(1440)$	$^2 8_{1/2}[56, 0^+]_{(1,0);0}$	398	$108 \chi_1^2$	$227 \pm 67$
$P_{11}$	$N(1710)$	$^2 8_{1/2}[70, 0^+]_{(0,1);0}$	587	$173 \chi_2^2$	$22 \pm 17$
$S_{31}$	$\Delta(1620)$	$^2 10_{1/2}[70, 1^-]_{(0,0);1}$	526	16	$37 \pm 11$
$P_{31}$	$\Delta(1910)$	$^4 10_{1/2}[56, 2^+]_{(0,0);0}$	716	42	$52 \pm 19$
$P_{33}$	$\Delta(1232)$	$^4 10_{3/2}[56, 0^+]_{(0,0);0}$	229	116	$119 \pm 5$
$P_{33}$	$\Delta(1920)$	$^4 10_{3/2}[56, 2^+]_{(0,0);0}$	723	22	$28 \pm 19$
$D_{33}$	$\Delta(1700)$	$^2 10_{3/2}[70, 1^-]_{(0,0);1}$	580	27	$45 \pm 21$
$D_{35}$	$\Delta(1930)$	$^2 10_{5/2}[70, 2^-]_{(0,0);1}$	729	0	$52 \pm 23$
$F_{35}$	$\Delta(1905)$	$^4 10_{5/2}[56, 2^+]_{(0,0);0}$	713	9	$36 \pm 20$
$F_{37}$	$\Delta(1950)$	$^4 10_{7/2}[56, 2^+]_{(0,0);2}$	741	45	$120 \pm 14$
$H_{3,11}$	$\Delta(2420)$	$^4 10_{11/2}[56, 4^+]_{(0,0);0}$	1023	12	$40 \pm 22$
$S_{31}$	$\Delta(1900)$	$^2 10_{1/2}[70, 1^-]_{(1,0);1}$	710	$2 \chi_1^2$	$38 \pm 21$
$P_{33}$	$\Delta(1600)$	$^4 10_{3/2}[56, 0^+]_{(1,0);0}$	513	$108 \chi_1^2$	$61 \pm 32$

Table VIII:  $\Delta\pi$  decay widths of (3 and 4 star) nucleon and delta resonances in MeV. For classification of the resonances see Table VII. The experimental values are taken from [17].

State	Mass	$k(\text{MeV})$	$l$	$\Gamma(\text{th})$	$\Gamma(\text{exp})$	$l$	$\Gamma(\text{th})$	$\Gamma(\text{exp})$
$S_{11}$	$N(1535)$	244				D	23	$1 \pm 1$
$S_{11}$	$N(1650)$	345				D	24	$7 \pm 5$
$P_{13}$	$N(1720)$	402	P	1	$102 \pm 89$	F	10	
$D_{13}$	$N(1520)$	230	S	3	$10 \pm 4$	D	9	$15 \pm 3$
$D_{13}$	$N(1700)$	386	S	111	$2 \pm 4$	D	114	$14 \pm 26$
$D_{15}$	$N(1675)$	366				D	123	$88 \pm 14$
$F_{15}$	$N(1680)$	370	P	2	$13 \pm 5$	F	3	$1 \pm 1$
$G_{17}$	$N(2190)$	740	D	13		G	12	
$G_{19}$	$N(2250)$	780				G	40	
$H_{19}$	$N(2220)$	760	F	3		H	3	
$I_{1,11}$	$N(2600)$	1003	G	4		I	3	
$P_{11}$	$N(1440)$	147				P	$0.1 \chi_1^2$	$87 \pm 30$
$P_{11}$	$N(1710)$	394				P	$70 \chi_2^2$	$41 \pm 33$
$S_{31}$	$\Delta(1620)$	320				D	89	$67 \pm 26$
$P_{31}$	$\Delta(1910)$	546	P	4				
$P_{33}$	$\Delta(1920)$	553	P	15		F	14	
$D_{33}$	$\Delta(1700)$	386	S	55	$112 \pm 53$	D	89	$12 \pm 10$
$D_{35}$	$\Delta(1930)$	560	P	0		F	0	
$F_{35}$	$\Delta(1905)$	542	P	18		F	27	
$F_{37}$	$\Delta(1950)$	575				F	36	$77 \pm 20$
$H_{3,11}$	$\Delta(2420)$	890				H	11	
$S_{31}$	$\Delta(1900)$	539				D	$\chi_1^2$	
$P_{33}$	$\Delta(1600)$	303	P	$25 \chi_1^2$	$180 \pm 143$	F	0	$16 \pm 25$

Table IX:  $N^* \rightarrow N\eta$  and  $\Delta^* \rightarrow \Delta\eta$  decay widths of (3 and 4 star) nucleon and delta resonances in MeV. For classification of the resonances see Table VII. The experimental values are taken from [17]. The mixing angle for the  $\eta$  mesons is  $\theta_P = -23^\circ$  [20].  $\chi_1$  and  $\chi_2$  are defined in the caption of Table I.

State	Mass	$k(\text{MeV})$	$\Gamma(\text{th})$	$\Gamma(\text{exp})$
$S_{11}$	$N(1535)$	182	0.1	$74 \pm 39$
$S_{11}$	$N(1650)$	346	8	$11 \pm 6$
$P_{13}$	$N(1720)$	420	0.2	
$D_{13}$	$N(1520)$	150	0.6	
$D_{13}$	$N(1700)$	400	4	
$D_{15}$	$N(1675)$	374	17	
$F_{15}$	$N(1680)$	379	0.5	
$G_{17}$	$N(2190)$	791	11	
$G_{19}$	$N(2250)$	831	9	
$H_{19}$	$N(2220)$	811	0.7	
$I_{1,11}$	$N(2600)$	1054	3	
$P_{11}$	$N(1710)$	410	$17\chi_2^2$	
$P_{31}$	$\Delta(1910)$	322	0.0	
$P_{33}$	$\Delta(1920)$	335	0.5	
$D_{35}$	$\Delta(1930)$	348	0	
$F_{35}$	$\Delta(1905)$	316	1	
$F_{37}$	$\Delta(1950)$	372	2	
$H_{3,11}$	$\Delta(2420)$	786	2	
$S_{31}$	$\Delta(1900)$	309	$3\chi_1^2$	

Table X: Strong decay widths for  $\Delta^* \rightarrow N + \pi$  and  $N^* \rightarrow N + \pi$  in MeV. Experimental values are from [17].

Resonance	$L$	$\Gamma(\text{th})$				$\Gamma(\text{exp})$
		Ref. [15]	Ref. [11]	Ref. [12]	Present	
$\Delta(1232)P_{33}$	0	70	121	108	116	$119 \pm 5$
$\Delta(1950)F_{37}$	2	27	56	50	45	$120 \pm 14$
$\Delta(2420)H_{3,11}$	4	4		8	12	$40 \pm 22$
$\Delta(2950)K_{3,15}$	6	1		3	5	$13 \pm 8$
$N(1520)D_{13}$	1		85	74	115	$67 \pm 9$
$N(2190)G_{17}$	3			48	34	$67 \pm 27$
$N(2600)I_{1,11}$	5			11	9	$49 \pm 20$

Table XI: Strong decay widths for the missing nucleon and delta resonances below 2 GeV. The mixing angle for the  $\eta$  mesons is  $\theta_P = -23^\circ$  [20].

State	Mass	Resonance	$\Gamma(\text{MeV})$			
			$N\pi$	$\Delta\pi$	$N\eta$	$\Delta\eta$
$P_{1,2J}$	$N(1720)$	${}^28_J[20, 1^+]_{(0,0);0}$	0	0	0	
$D_{1,2J}$	$N(1875)$	${}^28_J[70, 2^-]_{(0,0);1}$	0	0	0	
$P_{13}$	$N(1875)$	${}^28_{3/2}[70, 2^+]_{(0,0);2}$	56	56	9	
$F_{15}$	$N(1875)$	${}^28_{5/2}[70, 2^+]_{(0,0);2}$	85	43	19	
$S_{11}$	$N(1972)$	${}^48_{1/2}[70, 2^-]_{(0,0);1}$	0	0	0	
$D_{13}$	$N(1972)$	${}^48_{3/2}[70, 2^-]_{(0,0);1}$	0	0	0	
$D_{15}$	$N(1972)$	${}^48_{5/2}[70, 2^-]_{(0,0);1}$	0	0	0	
$G_{17}$	$N(1972)$	${}^48_{7/2}[70, 2^-]_{(0,0);1}$	0	0	0	
$P_{11}$	$N(1972)$	${}^48_{1/2}[70, 2^+]_{(0,0);2}$	19	15	17	
$P_{13}$	$N(1972)$	${}^48_{3/2}[70, 2^+]_{(0,0);2}$	9	94	9	
$F_{15}$	$N(1972)$	${}^48_{5/2}[70, 2^+]_{(0,0);2}$	4	156	4	
$F_{17}$	$N(1972)$	${}^48_{7/2}[70, 2^+]_{(0,0);2}$	18	96	20	
$S_{11}$	$N(1909)$	${}^28_{1/2}[70, 1^-]_{(1,0);1}$	$22 \chi_1^2$	$0.7 \chi_1^2$	$0.5 \chi_1^2$	
$D_{13}$	$N(1909)$	${}^28_{3/2}[70, 1^-]_{(1,0);1}$	$28 \chi_1^2$	$0.6 \chi_1^2$	$\chi_1^2$	
$P_{13}$	$N(1815)$	${}^48_{3/2}[70, 0^+]_{(0,1);0}$	$30 \chi_2^2$	$211 \chi_2^2$	$24 \chi_2^2$	
$S_{11}$	$N(1866)$	${}^28_{1/2}[56, 1^-]_{(0,1);1}$	$211 \chi_2^2$	$84 \chi_2^2$	$4 \chi_2^2$	
$D_{13}$	$N(1866)$	${}^28_{3/2}[56, 1^-]_{(0,1);1}$	$271 \chi_2^2$	$71 \chi_2^2$	$7 \chi_2^2$	
$P_{1,2J}$	$N(1997)$	${}^28_J[70, 1^+]_{(0,1);0}$	0	0	0	
$S_{11}$	$N(1997)$	${}^28_{1/2}[70, 1^-]_{(0,1);1}$	$3 \chi_2^2$	$34 \chi_2^2$	$5 \chi_2^2$	
$D_{13}$	$N(1997)$	${}^28_{3/2}[70, 1^-]_{(0,1);1}$	$3 \chi_2^2$	$30 \chi_2^2$	$7 \chi_2^2$	
$D_{33}$	$\Delta(1945)$	${}^210_{3/2}[70, 2^-]_{(0,0);1}$	0	0	0	
$F_{33}$	$\Delta(1945)$	${}^210_{3/2}[70, 2^+]_{(0,0);2}$	9	105	4	
$F_{35}$	$\Delta(1945)$	${}^210_{5/2}[70, 2^+]_{(0,0);2}$	13	83	2	
$D_{33}$	$\Delta(1977)$	${}^210_{3/2}[70, 1^-]_{(1,0);1}$	$5 \chi_1^2$	$7 \chi_1^2$	$3 \chi_1^2$	
$F_{31}$	$\Delta(1786)$	${}^210_{1/2}[70, 0^+]_{(0,1);0}$	$27 \chi_2^2$	$172 \chi_2^2$	0.0	

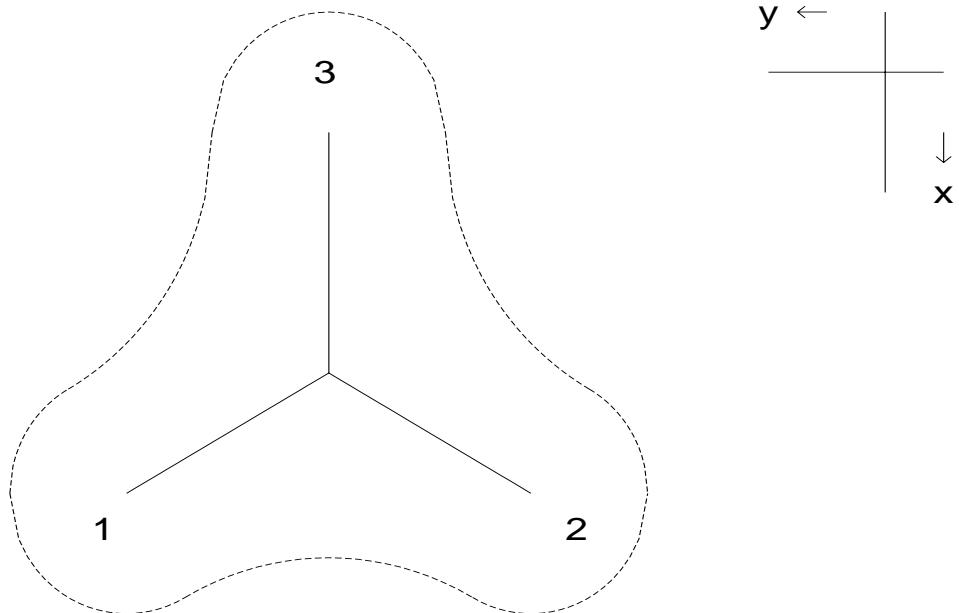


Figure 1: Collective model of baryons.



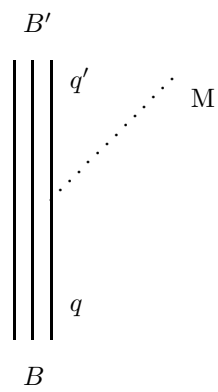


Figure 2: Elementary meson emission.

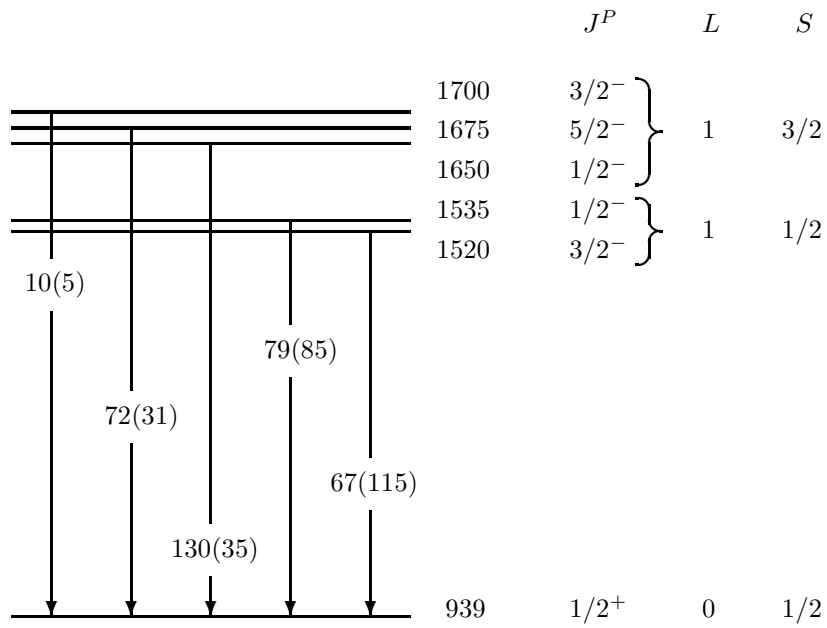


Figure 3: Strong decay widths for  $N^* \rightarrow N + \pi$  decays of negative parity resonances with  $L^P = 1^-$ . The theoretical values are in parenthesis. All values in MeV.

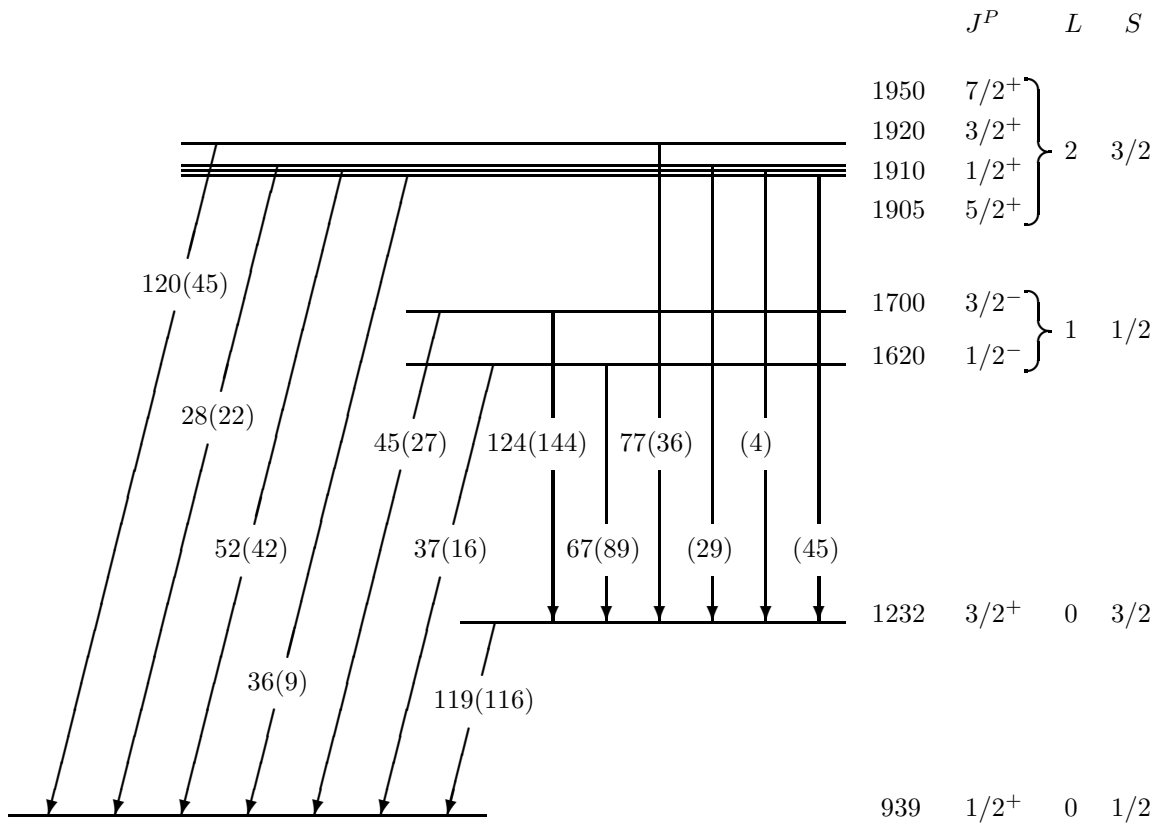


Figure 4: Strong decay widths for  $\Delta^* \rightarrow N + \pi$  and  $\Delta^* \rightarrow \Delta + \pi$  decays of positive parity resonances with  $L^P = 2^+$  and negative parity resonances with  $L^P = 1^-$ . Notation as in Fig. 3.